FEMS Microbes, 2024, 5, xtae014
DOI: 10.1093/femsmc/xtae014
Advance access publication date: 7 May 2024
Research Article – Microbes & Disease

Colonization of vancomycin-resistant *Enterococcus faecium* in human-derived colonic epithelium: unraveling the transcriptional dynamics of host–enterococcal interactions

Paul B. Stege [1], Jeffrey M. Beekman[2,3], Antoni P. A. Hendrickx[4], Laura van Eijk[1], Malbert R. C. Rogers[1], Sylvia W. F. Suen[2,3], Annelotte M. Vonk[2,3], Rob J. L. Willems[1], Fernanda L. Paganelli [1,5,*]

[1]Department of Medical Microbiology, UMC Utrecht, Utrecht, 3584CX, The Netherlands
[2]Department of Pediatric Pulmonology, Wilhelmina Children's Hospital, University Medical Center Utrecht, Utrecht University, Utrecht, 3584CX, The Netherlands
[3]Regenerative Medicine Utrecht, University Medical Center Utrecht, Utrecht University, Utrecht, 3584CX, The Netherlands
[4]Centre for Infectious Disease Control, National Institute for Public Health and the Environment (RIVM), 3721MA, The Netherlands
[5]Winclove Probiotics, Amsterdam, 1033JS, The Netherlands
*Corresponding author. Tt. Vasumweg 221, 1033 SJ Amsterdam, The Netherlands. E-mail: f.paganelli@winclove.nl
Editor: [Julia Willett]

Abstract

Enterococcus faecium is an opportunistic pathogen able to colonize the intestines of hospitalized patients. This initial colonization is an important step in the downstream pathogenesis, which includes outgrowth of the intestinal microbiota and potential infection of the host. The impact of intestinal overgrowth on host–enterococcal interactions is not well understood. We therefore applied a RNAseq approach in order to unravel the transcriptional dynamics of *E. faecium* upon co-culturing with human derived colonic epithelium. Co-cultures of colonic epithelium with a hospital-associated vancomycin resistant (vanA-type) *E. faecium* (VRE) showed that VRE resided on top of the colonic epithelium when analyzed by microscopy. RNAseq revealed that exposure to the colonic epithelium resulted in upregulation of 238 VRE genes compared to the control condition, including genes implicated in pili expression, conjugation (plasmid_2), genes related to sugar uptake, and biofilm formation (chromosome). In total, 260 were downregulated, including the *vanA* operon located on plasmid_3. Pathway analysis revealed an overall switch in metabolism to amino acid scavenging and reduction. In summary, our study demonstrates that co-culturing of VRE with human colonic epithelium promotes an elaborate gene response in VRE, enhancing our insight in host–*E. faecium* interactions, which might facilitate the design of novel anti-infectivity strategies.

Keywords: resistant; *Enterococcus faecium*; epithelium; plasmids; gene expression; RNAseq

Introduction

Vancomycin resistant *Enterococcus faecium* (VRE) emerged as an important opportunistic pathogen and is recognized by the World Health Organization (WHO) as a global threat (WHO 2017). In hospital settings, VREs are able to colonize the intestines of patients, followed by rapid outgrowth, which puts patients at risk of self-contamination during common hospital procedures, and subsequent bacteraemia (de Regt et al. 2008, Ubeda et al. 2010, Ruiz-Garbajosa et al. 2012, Taur et al. 2012, Chilambi et al. 2020). While enterococci are minority species in a healthy microbiota, accounting for <0.1% of intestinal microbiota, these numbers can significantly increase in hospitalized patients where *E. faecium* can even represent the majority bacterial species in the intestines (Magruder et al. 2019). Extensive molecular epidemiological and comparative genomic analyses revealed that *E. faecium* strains from hospitalized patients are part of a distinct phylogenetic clade that was initially designated clonal complex-17 and later renamed clade A1 (Willems et al. 2005, Lebreton et al. 2013, Arredondo-Alonso et al. 2020). *Enterococcus faecium* genes unique to clade A1 include putative virulence genes, genes encoding antibiotic transport, intestinal colonization factors, and genes implicated in carbohydrate metabolism particularly indicating a shift to the utilization of amino sugars, like those that occur on cell surfaces and in mucin (Lebreton et al. 2013). Plasmidome analyses indicated that the predicted plasmidome size of isolates from hospitalized patients was considerably larger than that from other isolation sources, such as non-hospitalized persons, dogs, pigs, and poultry (Arredondo-Alonso et al. 2020). Plasmid encoded genes specific for isolates from hospitalized patients include a locus of three genes putatively encoding an ABC transport system with similarity to lipoprotein/bacteriocin/macrolide export systems, a bacteriocin gene with homology to *bacA*, and a complete phosphotransferase system (PTS) putatively involved in carbohydrate uptake (Zhang et al. 2013). The acquisition and enrichment of specific carbohydrate uptake systems in clade A1 strains may provide these isolates a broader and or novel metabolic repertoire allowing clade A1 *E. faecium* to colonize the dysbiotic intestinal microbiota of hospitalized patients (Zhang et al. 2013). In fact, disruption of the intestinal microbial community in hospitalized patients is thought to be one of the key factors contributing to the outgrowth of *E. faecium* in

Received 31 January 2024; **revised** 27 March 2024; **accepted** 6 May 2024

hospitalized patients (Ubeda et al. 2010, Stein-Thoeringer et al. 2019). Antibiotic-driven dysbiosis in the mammalian host does not only leads to *Enterococcus* outgrowth, it also results in changes in the architecture of the intestinal epithelial cell lining. In an intestinal colonization model in mice, antibiotic treatment allowing enterococcal outgrowth resulted in a reduction of the mucus-associated intestinal microbiota layer, colon wall, and Muc-2 mucus layer, as well as deformation of E-cadherin adherens junctions between colonic cells and entrapment of *E. faecium* in an extracellular matrix consisting of secretory IgA, polymeric immunoglobulin receptor, and epithelial cadherin (E-cadherin) proteins (Hendrickx et al. 2015).

Together, these findings suggest that particular genes acquired by hospital-associated *E. faecium* strains facilitate intestinal colonization especially in hospitalized patients and result in significant changes in the intestinal architecture. However, detailed insights on *E. faecium* host interaction in the human intestines are still largely lacking. Recently, human-derived colonic organoids have been used as an *ex vivo* model to study human specific bacteria–host interactions. Differentiated colonic organoids, grown as monolayers of colonic epithelium, express several cell types, including colonocytes, Lgr5+ stem cells, mucus-producing goblet cells, and important cell structures like occludin and E-cadherin (Jung et al. 2011, Zachos et al. 2016, McClintock et al. 2020). In this study, we applied an RNA sequencing approach to unravel *E. faecium*-host transcriptional responses during experimental *in vitro* colonization of human-derived colonic epithelium. Our findings highlight important transcriptional changes of *E. faecium* that may play an important role during intestinal colonization, which enhances our insight in host–*E. faecium* interactions.

Methods

Organoid line and growth conditions

The clonal human-derived colonic organoid cell line Pt15-70206 was used to grow colonic epithelium according to the protocol described by Vonk et al. (2020). In brief, a colonic organoid stock was thawed and organoids were cultured in domes of Matrigel covered by medium containing 15% Advanced DMEM/F12, 1x Glutamax, 100 U/ml Penicillin-Streptomycin, 10 mmol/l HEPES (all Invitrogen), 25% Rspo1 Conditioned Medium, 10% Noggin Conditioned Medium (conditioned medium was home-made), 2% B27 (Invotrogen), 1.25 mM N-acetylcysteine, 10 mM Nicotinamide, 10 μM p38 inhibitor SB202190 (all Sigma-Aldrich), 50 ng/ml mEGF (Invitrogen), 0.5 μM A83–01 (Tocris), 50% Wnt-3A Conditioned Medium (WCM). After on average 13 passages, organoids were disrupted and used to seed transwells and generate confluent colonic epithelium. During the first 24 h in transwells, medium was supplemented with 10 nM rock inhibitor Y-27632 (Selleck Chemicals). Once the TEER surpassed 100 ohm/cm^2, the culture medium was replaced by culture medium lacking WCM, nicotinamide, and p38 inhibitor, called differentiation medium (Zomer-van Ommen et al. 2018). Differentiation medium was refreshed 24 h before the inoculation of co-cultures by differentiation medium without added Penicillin–Streptomycin, to prevent inhibition of bacterial growth. All experiments were performed in accordance with relevant ethical guidelines and regulations.

Bacterial strain and growth conditions

The vancomycin (vanA-type, ST117) resistant *E. faecium* strain E8202 was previously isolated from a patient via a rectal swab during a Dutch hospital outbreak in 2015. This strain was fully sequenced and assembled and contains a total of six plasmids (Arredondo-Alonso et al. 2020). *Enterococcus faecium* E8202 is used throughout this study except for the confocal live imaging experiment in which the hospital-derived *E. faecium* strain E745 was used (Arredondo-Alonso et al. 2020, Top et al. 2020). Sequences were annotated using Prokka version 1.10 and operon-mapper with default settings (Seemann 2014, Taboada et al. 2018). Annotation was further expanded by blasting genes manually, applying a 98% identity cut-off. Bacteria were initially cultured at 37°C and shaking at 150 rpm in Brain Heart Infusion broth to an OD600 of 0.4. After a washing step in PBS, bacteria were resuspended in organoid culture media and concentrated to an artificial OD600nm of 0.6. These cultures were subsequently used for co-cultures with colonic epithelium, applying a multiplicity of infection of 6. Co-cultures were spun down at 250 × *g* for 5 min to ensure cell contact and used for 24 h co-culture at 37°C and 5% CO_2.

Confocal live imaging

Co-culture of a colonic epithelium and *E. faecium* were analysed for fluorescence using confocal live imaging with a confocal laser microscope (Leica SP5) and a Plan Apo 40x objective (numerical aperture of 0.85). Only for this experiment, the vancomycin (vanA-type) resistant *E. faecium* strain E745 was used as we were not able to generate a GFP producing strain E8202 (Zhang et al. 2017). A constitutively GFP expressing plasmid was constructed by ordering a gblock containing a strong bacillus promotor (P*groE*) and the free-use GFP (Integrated DNA Technologies) (Jiao et al. 2017, N Coleman 2019). This gblock was then digested and ligated with pWS3-msrC-Pbac-T7 using the *ApaI* and *SmaI* restriction sites located on both the plasmid as gblock (de Maat et al. 2019). The resulting plasmid was then used to transform *E. faecium* strain E745 in order to constitutively express GFP in confocal microscopy. GFP was excited at 488 nm, Alexa Fluor 647-conjugated wheat germ agglutinin (WGA) (ThermoFisher Scientific) was excited at 633 nm, and Alexa Fluor 405-conjugated phalloidin (Thermo Fisher Scientific) at 405 nm. Pictures were analysed with LAS AF software (Leica).

RNA extraction and RNA sequencing

RNA extraction was performed according to a modified protocol of the RNeasy Mini Kit (Qiagen). First, 80% of the media in the upper compartment of transwells was slowly removed. Cells were then resuspended in 200 µl RLT buffer, transferred to 2 ml bead beat tubes (0.5 ml glass 0.1 mm beads, Sigma-Aldrich), and snap frozen in liquid nitrogen. Beat beating was applied at 3800 rpm for 1 min, followed by 1 min incubation on ice and two additional rounds of beat beating, using the Mini-Beadbeater-24 (Biospec). The RNeasy Mini Kit protocol was then resumed at the ethanol addition step. The recommended DNases treatment was applied during RNA extraction, followed by an additional DNase treatment (TURBO DNA-free kit, Ambion). Total RNA was quantified by Qubit assay (Invitrogen). Samples were sent to the Utrecht Sequencing Facility (USEQ; http://useq.nl) for rRNA removal using the TruSeq Stranded mRNAn kit (Illumina) for replicates 1–3 and the Stranded Total RNA Library Prep for replicates 4–6, due to discontinuation of the rRNA removal kit. The NextSeq500 (Illumina) was used, with high output and single-end sequencing of 1×75 bp (Illumina) and the company protocol/standard settings (USEQ).

Data processing and analysis

Sequence data were trimmed using Trim Galore version 0.6.4 with standard settings. The human genome (Ensembl release 99, chromosome 1–22, X, Y, MT) was merged to the genome of *E. faecium* E8202 and used to create a database with STAR version 2.7.9a using standard settings and *-sjdbOverhang* 49 (Dobin et al. 2013). Sequence data were subsequently aligned to STAR with standard settings and *-quantMode GeneCounts*. The resulting list of aligned genes was split into two parts; analysis of the host response and pathogen response. Analysis of sequencing data were performed in R version 4.0 and the functions of the packages ggplot2 (Wickham 2016, R Core Team 2020). Genes with a low number of read counts were removed to suppress sequencing noise using the condition: *rowSums*(*counts*(*df*) >= 5) >= 6. This results in remaining genes with at least 5 read counts per 6 samples. DESeq2 version 1.30 was then used for the analysis of differentially expressed genes, while applying batch correction (Love et al. 2014). Apeglm shrinkage estimator version 1.14 was subsequently applied, effectively accounting for genes with extremely low expression levels, among other expression ranges (Fig. S1) (Zhu et al. 2019). A cut-off of adjusted *P*-values .05 and a fold change of 1.5 were applied to distinguish differentially expressed genes. The top 50 upregulated and downregulated genes were determined based on the lowest adjusted *P*-values. Normalized read counts per sample were computed using DESeq2's size factor method and employed for visualizing the expression of these selected genes. For pathway analysis, genes were selected using a cutoff of adjusted *P*-values $\leq$ .1 and fold change $\geq$ 1.5. KEGG automatic annotation server was first applied to predict gene function (Moriya et al. 2007). Pathway analysis was subsequently performed using ClusterProfiler version 4.0, with 999 permutations and gene set size limitations of 8 and 100, respectively (Yu et al. 2012).

Comparative plasmid analysis

The Basic Local Alignment Search Tool (blastn at https://blast.ncbi.nlm.nih.gov/Blast.cgi, interrogated on 27 April 2023) was used to find plasmids with sequence similarity to *E. faecium* E8202 plasmid_2 (GenBank accession number LR135345.1) and plasmid_3 (GenBank accession number LR135346.1). For plasmids similar to E8202 plasmid_2 all 14 plasmids with a coverage >85% coverage and identity >95% were selected and downloaded (Table 1). A BLAST search using the thresholds (coverage >75%; identity >95%) was performed to identify plasmids similar to E8202 plasmid_3. This resulted in only two similar plasmids: *E. faecium* plasmid pUK040_2 and *E. faecium* plasmid p4_03A17012. Reducing coverage thresholds to >60% yielded 20 additional hits (Table 2). The 22 plasmid sequences displaying similarity to plasmid_3 were also downloaded. E8202 plasmid_2 and 3 GenBank files (LR135345.1 and LR135346.1, respectively) were uploaded in Proksee [https://proksee.c,a (Grant et al. 2023)]. Subsequently, FASTA files of identified plasmids similar to E8202 plasmid_2 or 3 (Tables 1 and 2) were uploaded and aligned to the E8202 plasmids using the BLAST Sequence comparison tool in Proksee. Aligned plasmids were visualized in Proksee. PlasmidFinder2.1 (https://cge.food.dtu.dk/services/PlasmidFinder/, repA_N database, 100% identity based on PlasmidFinder; Software version: 2.0.1; Database version: (2023-01-18)) (Carattoli et al. 2014)) was used to identify plasmid encoded *rep* genes, and Pathogenwatch (https://pathogen.watch) was used to infer STs of the isolates carrying E8202 plasmid_2 and plasmid_3 similar plasmids.

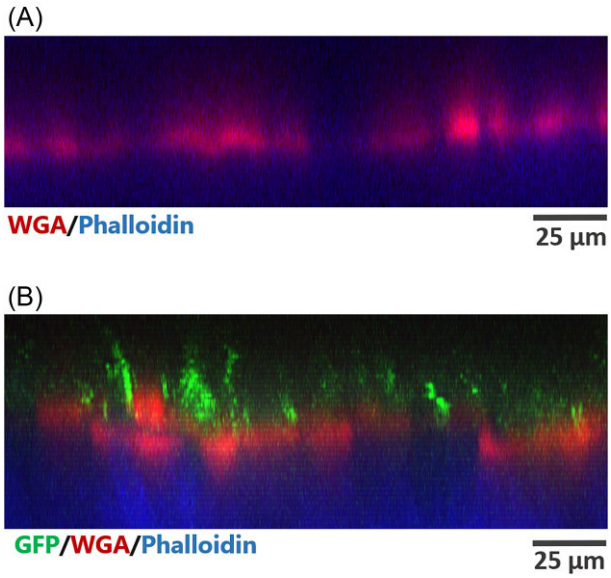

Figure 1. Co-cultures of colonic epithelium and *E. faecium* reveal spatial organization. (A) Colonic epithelium used for confocal live imaging, visualized by a side view of stacked images. (B) Confocal live imaging of co-culture consisting of colonic epithelium and a GFP expressing vancomycin-resistant *E. faecium* strain E745. Images are stacked to generate a side view of the co-cultures. Actin was stained by phalloidin (in blue), mucus was stained by WGA (in red), and *E. faecium* expressed GFP (in green).

Results

Establishing *E. faecium*-human colonic epithelium co-cultures

To study *E. faecium*–host interaction, we first cultured human derived colonic differentiated epithelium. Using confocal live imaging, we visualized both the colonic epithelium and a mucus layer (Fig. 1A). We then continued to co-culture the vanA-type vancomycin-resistant *E. faecium* strain E8202 for 24 h with colonic differentiated epithelium. This strain was isolated from a hospitalized patient in 2015 and using full genome assembly, was determined to belong to clade A1 (ST117) and containing 6 plasmids (Table S1) (Arredondo-Alonso et al. 2020). We first established that this *E. faecium* strain was able to grow in both the cell culture medium (i.e. control condition) as well as in the co-culture with colonic epithelium (Fig. S2). We then continued to visualize the spatial organization of the co-cultures using confocal live imaging. For this purpose, we used the modified vancomycin-resistant *E. faecium* strain E745 that continuously expressed Green fluorescence Protein (GFP) and co-cultured with colonic epithelium. *Enterococcus faecium* strain E8202 did not accept the GFP expression plasmid upon transformation, which is why we were forced to use this second *E. faecium* strain. *Enterococcus faecium* strain E745 is also a vanA-type vancomycin-resistant strain, recovered from a hospitalized patient in 2000, and also belongs to clade A1 (ST16) (Zhang et al. 2017). We observed that *E. faecium* E745 resided on top of the colonic epithelium, rather than being positioned between colonic cells (Fig. 1B). It was unclear if *E. faecium* and the colonic cells were in direct contact or separated by the mucus layer.

Transcriptome of colonic epithelium during colonization with *E. faecium* E8202

We next investigate the transcriptional response of colonic epithelium upon co-culturing with *E. faecium* E8202 by performing

Table 1. Plasmids similar to E8202 plasmid_2.

Nr	Accesion	url	Size (bp)	Description	Plasmid name	Replicon Match ID	Contig Inc type	% coverage of E8202 plasmid 2	% identity with E8202 plasmid 2	Strain name	Strain ST	Strain source	Strain isolation site	Institute	City	Country	Strain year	Van res	Van gene	Lit plasmid
0	LR135345.1	https://www.ncbi.nlm.nih.gov/datasets/genome/GCF_900639535.1/	188 833	*Enterococcus faecium* isolate E8202 genome assembly, plasmid: 2	E8202_plasmid_2	repUS15_1	RepA_N	ND	ND	E8202	117	Hosp patient	0	Isala klinieken Zwolle	Zwolle	The Netherlands	2015	1	vanA	https://pubmed.ncbi.nlm.nih.gov/32047136/
1	LR135340.1	https://www.ncbi.nlm.nih.gov/datasets/genome/GCF_900639505.1/	234 907	*Enterococcus faecium* isolate E7356 genome assembly, plasmid: 2	E7356_plasmid_2	repUS15_1	RepA_N	100	99.95	E7356	117	Hosp patient	Faeces	Canisius WZ Nijmegen	Nijmegen	The Netherlands	2012	1	vanB	https://pubmed.ncbi.nlm.nih.gov/32047136/
2	CP046167.1	https://www.ncbi.nlm.nih.gov/datasets/genome/GCF_016864255.1/	234 807	*Enterococcus faecium* strain WGS1811-4-7 plasmid unnamed1, complete sequence	WGS1811-4-7 plasmid unnamed1	repUS15_1	RepA_N	99	99.98	WGS1811-4-7	117	Hosp patient	Clin_Site_Other	Haukeland University Hospital	Bergen	Norway	2017			
3	CP018066.1	https://www.ncbi.nlm.nih.gov/datasets/genome/GCF_001886635.1/	230 049	*Enterococcus faecium* strain E1 plasmid pE1_230, complete sequence	pE1_230	repUS15_1	RepA_N	97	99.94	E1	117	Hosp patient	Blood	Hospital Ramon y Cajal	Madrid	Spain	2016			https://www.ncbi.nlm.nih.gov/pmc/articles/PMC5374248/
4	CP044275.1	https://www.ncbi.nlm.nih.gov/datasets/genome/GCF_008728475.1/	201 015	*Enterococcus faecium* strain V2937 plasmid pHVH-V2937-1, complete sequence	pHVH-V2937-1	repUS15_1	RepA_N	94	99.99	V2937	117	Hosp patient	Pus	Hvidovre Hospital	Copenhagen	Denmark	2018			https://pubmed.ncbi.nlm.nih.gov/32125377/
5	LR135198.1	https://www.ncbi.nlm.nih.gov/datasets/genome/GCF_900639345.1/	223 834	*Enterococcus faecium* isolate E6055 genome assembly, plasmid: 2	E6055_plasmid_2	repUS15_1	RepA_N	93	99.92	E6055	18	Hosp patient	Faeces	Hospital Santo Antonio	Porto	Portugal	2010	1	vanA	https://pubmed.ncbi.nlm.nih.gov/32047136/
6	CP063599.1	https://www.ncbi.nlm.nih.gov/datasets/genome/GCA_022811325.1/	184 907	*Enterococcus faecium* strain BMT-3-2-1 plasmid pHJB-2-1_01, complete sequence	pHJB-2-1_01	repUS15_1	RepA_N	90	99.99	BMT-3-2-1	889	Hosp patient	Clin_Site_Other	University Medical Center Hamburg-Eppendorf	Hamburg	Germany	2015			https://www.sciencedirect.com/science/article/pii/S2213716522000315?via%3Dihub
7	CP063605.1	https://www.ncbi.nlm.nih.gov/datasets/genome/GCA_022811345.1/	184 904	*Enterococcus faecium* strain BMT-2-3-8 plasmid pSS-3-8_01, complete sequence	pSS-3-8_01	repUS15_1	RepA_N	90	99.98	BMT-2-3-8	117	Hosp patient	Clin_Site_Other	University Medical Center Hamburg-Eppendorf	Hamburg	Germany	2014			https://www.sciencedirect.com/science/article/pii/S2213716522000315?via%3Dihub
8	LR135365.1	https://www.ncbi.nlm.nih.gov/datasets/genome/GCF_900639565.1/	221 376	*Enterococcus faecium* isolate E8195 genome assembly, plasmid: 2	E8195_plasmid_2	repUS15_1	RepA_N	87	99.99	E8195	117	Hosp patient	0	ZGT Almelo	Almelo	The Netherlands	2014	0	None	https://pubmed.ncbi.nlm.nih.gov/32047136/
9	OU015709.1	https://www.ncbi.nlm.nih.gov/datasets/genome/GCF_907165365.1/	238 492	*Enterococcus faecium* isolate USZ_VRE32_P32 genome assembly, plasmid: pl1	VRE32_P32_plasmid_pl1	repUS15_1	RepA_N	87	99.98	VRE32_P32	117	Hosp patient	Clin_Site_Other	University of Zurich	Zurich	Switserland	2021			
10	LR135298.1	https://www.ncbi.nlm.nih.gov/datasets/genome/GCF_900639465.1/	232 499	*Enterococcus faecium* isolate E7429 genome assembly, plasmid: 2	E7429_plasmid-2	repUS15_1	RepA_N	86	99.99	E7429	117	Hosp patient	Clin_Site_Other	UMCG	Groningen	The Netherlands	2010	1	vanB	https://pubmed.ncbi.nlm.nih.gov/32047136/
11	LR135402.1	https://www.ncbi.nlm.nih.gov/datasets/genome/GCF_900639595.1/	239 811	*Enterococcus faecium* isolate E8377 genome assembly, plasmid: 2	E8377_plasmid_2	repUS15_1	RepA_N	86	99.99	E8377	117	Hosp patient	0	MST	Enschede	The Netherlands	2015	1	vanB	https://pubmed.ncbi.nlm.nih.gov/32047136/
12	LR135395.1	https://www.ncbi.nlm.nih.gov/datasets/genome/GCF_900639605.1/	239 811	*Enterococcus faecium* isolate E8290 genome assembly, plasmid: 2	E8290_plasmid_2	repUS15_1	RepA_N	86	99.99	E8290	117	Hosp patient	0	MST	Enschede	The Netherlands	2015	1	vanB	https://pubmed.ncbi.nlm.nih.gov/32047136/
13	LR135415.1	https://www.ncbi.nlm.nih.gov/datasets/genome/GCF_900639615.1/	239 811	*Enterococcus faecium* isolate E8328 genome assembly, plasmid: 2	E8328_plasmid_2	repUS15_1	RepA_N	86	99.99	E8328	117	Hosp patient	0	MST	Enschede	The Netherlands	2015	0	None	https://pubmed.ncbi.nlm.nih.gov/32047136/
14	LR135409.1	https://www.ncbi.nlm.nih.gov/datasets/genome/GCF_900639625.1/	239 811	*Enterococcus faecium* isolate E8284 genome assembly, plasmid: 2	E8284_plasmid_2	repUS15_1	RepA_N	86	99.99	E8284	117	Hosp patient	0	MST	Enschede	The Netherlands	2015	1	vanB	https://pubmed.ncbi.nlm.nih.gov/32047136/

Table 2. Plasmids similar to E8202 plasmid_3.

Nr	Accesion	url	Size (bp)	Description	Plasmid name	Rep name	Rep family	Rep note	Rep name_2	Rep family_2	Rep note_2	Rep name_3	Rep family_3	Rep note_3	Rep name_4	Rep family_4	Rep note_4	% coverage of E8202 plasmid 3	% identity with E8202 plasmid 3	Strain name	Strain ST	Strain source	Strain isolation site	Institute	City	Country	Strain year	Van res	Van gene	Lit plasmid
0	NZ_LR135346.1	https://www.ncbi.nlm.nih.gov/datasets/genome/GCF_900639535.1/	40 152	Enterococcus faecium E8202 plasmid 3	E8202 plasmid 3	rep2_1	Inc18	pRE25										100	100	E8202	117	Hosp patient	0	Isala klinieken Zwolle	Zwolle	The Netherlands	2015	1	vanA	https://pubmed.ncbi.nlm.nih.gov/32047136/
1	NZ_CP091579.1	https://www.ncbi.nlm.nih.gov/datasets/genome/GCF_021899455.1/	44 472	Enterococcus faecium UK40 plasmid pUK040_2	pUK040_2	rep2_1	Inc18	pRE25										99	99.99	UK40	80	Human	rectal swab			Germany	2018	1	vanA	
2	NZ_CP046078.1	https://www.ncbi.nlm.nih.gov/datasets/genome/GCF_009697285.1/	36 877	Enterococcus faecium VRE plasmid p4_03A17012	p4_03A17012	rep17_2	RepA_N	pRUM_p29	rep1	Inc18	repR(pGB354)							77	99.95	VRE	NEW (clade A1)	Hosp patient	Blood		Calgary	Canada	2017	1	vanA	
3	NZ_LR135200.1	https://www.ncbi.nlm.nih.gov/datasets/genome/GCF_900639345.1/	41 060	Enterococcus faecium E6055 plasmid 4	E6055 plasmid 4	rep17_2	RepA_N	pRUM_p29	rep1	Inc18	repR(pGB354)							69	99.95	E6055	18	Hosp patient	Faeces	Hospital Santo Antonio	Porto	Portugal	2010	1	vanA	https://pubmed.ncbi.nlm.nih.gov/32047136/
4	NZ_LR962268.1	https://www.ncbi.nlm.nih.gov/datasets/genome/GCF_905121835.1/	88 201	Enterococcus faecalis 27 725_1#12 plasmid 2	27 725_1#12 plasmid 2	rep2	Inc18	pRE25	rep7a	Rep_Trans	pRE25	rep8b	RepA_N	repA(pEJ97p1)	repUS12	Rep1	repB(SAP014A)	68	99.99	27 725_1#12	6 (E. faecalis)	Hosp patient		UMC Utrecht	Utrecht	The Netherlands	2020	1	vanA	
5	NZ_CP083922.1	https://www.ncbi.nlm.nih.gov/datasets/genome/GCF_020162175.1/	52 056	Enterococcus faecium V1164 plasmid pV1164-2	pV1164-2	rep2	Inc18	pRE25	rep1	Inc18	repE(pAMbeta)	rep7a	Rep_Trans	pRE25				66	99.98	V1164	18	Hosp patient	Drain fluid	Hvidovre Hospital	Copenhagen	Denmark	2019	1	vanA	https://pubmed.ncbi.nlm.nih.gov/35922088/
6	NZ_LR135374.1	https://www.ncbi.nlm.nih.gov/datasets/genome/GCF_900639555.1/	88 799	Enterococcus faecium E8172 plasmid 3	E8172 plasmid 3	rep17_2	RepA_N		rep1	Inc18								66	99.95	E8172	80	Hosp patient	0	UMC Utrecht	Utrecht	The Netherlands	2014	1	vanA	https://pubmed.ncbi.nlm.nih.gov/32047136/
7	NZ_CP043327.1	https://www.ncbi.nlm.nih.gov/datasets/genome/GCF_007999025.2/	60 228	Enterococcus durans VREdu plasmid pSULI	pSULI	rep2	Inc18	pRE25	rep22	Rep1	repU(pKKS825)	repUS12	Rep1	repB(SAP014A)				66	99.99	VREdu	ND	Chicken	Chicken meat	University of Copenhagen	Copenhagen	Denmark	2015	1	vanA	
8	NZ_CP065756.1	https://www.ncbi.nlm.nih.gov/datasets/genome/GCF_018516925.1/	56 729	Enterococcus faecium 18-276 p18-276_2	p18-276_2	rep1	Inc18	repR (pGB354)	rep18b	Rep3	BO23315710 (pE1p13)							65	100	18-276	80	Hosp patient	Rectal swab	Centre Hospitalier Sud Francilien	Corbeil-Essonnes	France	2018	1	vanA	https://pubmed.ncbi.nlm.nih.gov/33895846/
9	NZ_OU015711.1	https://www.ncbi.nlm.nih.gov/datasets/genome/GCF_907165365.1/	51 289	Enterococcus faecium USZ_VRE32_P32 pl2	USZ_VRE32_P32 pl 2	rep2	Inc18	pRE25	rep7a	Rep_Trans	pRE25							64	99.99	VRE32_P32	117	Hosp patient	Inguinal/ rectal swab	University Hospital of Zurich (USZ)	Zurich	Switzerland	2017	1	vanA	https://www.ncbi.nlm.nih.gov/pmc/articles/PMC9040824/
10	LR135271.1	https://www.ncbi.nlm.nih.gov/search/all/?term=LR135271	17 934	Enterococcus faecium E7196 pl2	E7196 plasmid 2	rep17_2	RepA_N	pRUM_p29	rep1	Inc18	repR(pGB354)	rep14b	Rep_Trans	EMQU3221 (pQY003)				63	99.93	E7196	656	Hosp patient	Faeces	Henri Mondor	Creteil	France	2011	1	vanA	https://pubmed.ncbi.nlm.nih.gov/32047136/
11	NZ_CP027519.1	https://www.ncbi.nlm.nih.gov/datasets/genome/GCF_003020745.1/	48 209	Enterococcus faecium AUSMDU00004024 plasmid 2	AUSMDU00004024 plasmid 2	rep2	Inc18	pRE25	rep1	Inc18	repE(pAMbeta)	rep7a	Rep_Trans	pRE25				62	99.98	AUSMDU 00004024	203	Hosp patient	0		Victoria	Australia	2015	1	vanA	https://pubmed.ncbi.nlm.nih.gov/30189014/
12	NZ_CP060862.1	https://www.ncbi.nlm.nih.gov/datasets/genome/GCF_014490015.1/	49 122	Enterococcus faecium AML0157 plasmid pAML0157.1	pAML0157.1	rep2	Inc18	pRE25	rep1	Inc18	repE(pAMbeta)	rep7a	Rep_Trans	pRE25				62	99.98	AML0157	203	Hosp patient	Blood	University Hospital Cologne	Cologne	Germany	2016	1	vanA	https://pubmed.ncbi.nlm.nih.gov/33370443/
13	NZ_CP083914.1	https://www.ncbi.nlm.nih.gov/datasets/genome/GCF_020162155.1/	48 157	Enterococcus faecium isolate V1225 plasmid pV1225-2	pV1225-2	rep2	Inc18	pRE25	rep1	Inc18	repE(pAMbeta)	rep7a	Rep_Trans	pRE25				62	99.98	V1225	18	Hosp patient	Blood	Hvidovre Hospital	Copenhagen	Denmark	2019	1	vanA	https://pubmed.ncbi.nlm.nih.gov/35922088/
14	NZ_OU016029.1	https://www.ncbi.nlm.nih.gov/datasets/genome/GCF_907176815.1/	47 525	Enterococcus faecium USZ_VRE67_P60 plasmid: pl2	USZ_VRE67_P60 pl2	rep2	Inc18	pRE25	rep1	Inc18	repE(pAMbeta)	rep7a	Rep_Trans	pRE25				62	99.98	VRE67_P60	203	Hosp patient	Superficial wound	University Hospital of Zurich (USZ)	Zurich	Switzerland	2018	1	vanA	https://www.ncbi.nlm.nih.gov/pmc/articles/PMC9040824/
15	NZ_OU015948.1	https://www.ncbi.nlm.nih.gov/datasets/genome/GCF_907176135.1/	47 525	Enterococcus faecium USZ_VRE5_P5 plasmid: pl2	USZ_VRE5_P5 pl2	rep2	Inc18	pRE25	rep1	Inc18	repE(pAMbeta)	rep7a	Rep_Trans	pRE25				62	99.98	VRE5_P5	203	Hosp patient	Superficial wound	University Hospital of Zurich (USZ)	Zurich	Switzerland	2015	1	vanA	https://www.ncbi.nlm.nih.gov/pmc/articles/PMC9040824/
16	NZ_LR135491.1	https://www.ncbi.nlm.nih.gov/datasets/genome/GCF_900639715.1/	42 699	Enterococcus faecium E8414 plasmid 4	E8414 plasmid: 4	rep2	Inc18	pRE25	rep1	Inc18	repE(pAMbeta)							62	99.97	E8414	117	Hosp patient	0	Isala klinieken Zwolle	Zwolle	The Netherlands	2015	1	vanA	https://pubmed.ncbi.nlm.nih.gov/32047136/
17	NZ_OU016039.1	https://www.ncbi.nlm.nih.gov/datasets/genome/GCF_907177285.1/	47 525	Enterococcus faecium USZ_VRE53_P46 plasmid: pl2	USZ_VRE53_P46 pl2	rep2	Inc18	pRE25	rep1	Inc18	repE(pAMbeta)	rep7a	Rep_Trans	pRE25				62	99.99	VRE53_P46	203	Hosp patient	Superficial wound	University Hospital of Zurich (USZ)	Zurich	Switzerland	2018	1	vanA	https://www.ncbi.nlm.nih.gov/pmc/articles/PMC9040824/
18	NZ_LR962527.1	https://www.ncbi.nlm.nih.gov/datasets/genome/GCF_905122635.1/	72 911	Enterococcus faecalis 28 157_4#381 plasmid: 2	28 157_4#381 plasmid: 2	rep2	Inc18	pRE25	rep1	Inc18	pRE25							62	100	28 157_4#381	6 (E. faecalis)	Hosp patient	0	UMC Utrecht	Utrecht	The Netherlands	2020	1	vanA	
19	NZ_LR962419.1	https://www.ncbi.nlm.nih.gov/datasets/genome/GCF_905122345.1/	72 838	Enterococcus faecalis 28 157_4#218 plasmid: 2	28 157_4#218 plasmid: 2	rep2	Inc18	pRE25	rep1	Inc18	pRE25							62	100	28 157_4#218	6 (E. faecalis)	Hosp patient	0	UMC Utrecht	Utrecht	The Netherlands	2020	1	vanA	
20	NZ_CP020486.1	https://www.ncbi.nlm.nih.gov/datasets/genome/GCF_003071425.1/	49 542	Enterococcus faecium CFSAN059070 (VRE1589) plasmid 2	CFSAN059070 (VRE1589) plasmid 2	rep2	Inc18	pRE25	rep1	Inc18	repE(pAMbeta)	rep7a	Rep_Trans	pRE25				62	99.96	VRE1589	203	Hosp patient	Urine	Rigshospitalet	Copenhagen	Denmark	2014	1	vanA	https://www.ncbi.nlm.nih.gov/pmc/articles/PMC6211357/
21	AM932524.1	https://www.ncbi.nlm.nih.gov/nuccore/AM932524.1?report=genbank	34 616	Enterococcus faecium pIP816 BM4147 pIP816		rep2	Inc18	pRE25	rep1	Inc18	repE(pAMbeta)	rep7a	Rep_Trans	SAP108C001 (SAP108C)				61	99.99	BM4147	25	Hosp patient	Faeces			France	1986	1	vanA	https://www.nejm.org/doi/full/10.1056/NEJM198807213190307
22	CP066209.1	https://www.ncbi.nlm.nih.gov/datasets/genome/GCA_018517145.1/	32 413	Enterococcus faecium 18-204 plasmid p18-204_4	p18-204_4	rep17_2	RepA_N	pRUM_p29										61	100	18-204	18	Hosp patient	Rectal swab		Créteil	France	2018	1	vanA	https://pubmed.ncbi.nlm.nih.gov/33895846/

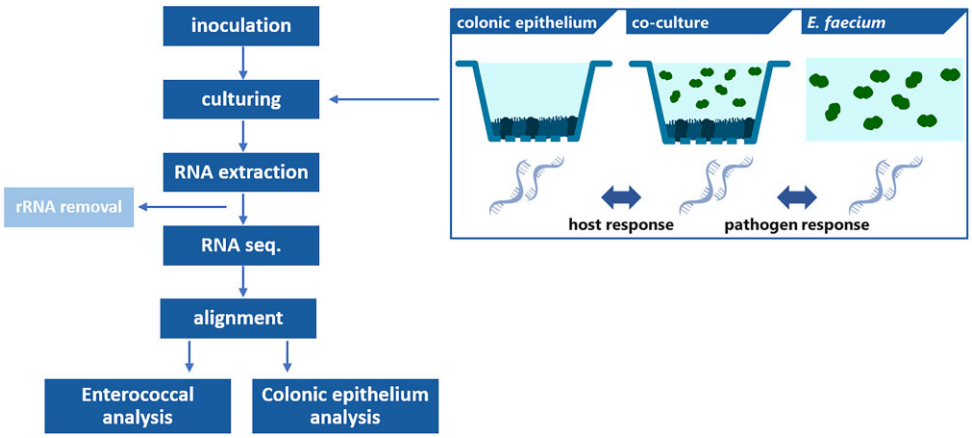

Figure 2. Schematic representation of culture conditions for RNA sequencing. To determine the host response and pathogen response, respectively, vancomycin resistant *E. faecium* strain E8202 and colonic epithelium were co-cultured and cultured separately in otherwise identical culture conditions for 24 h. Culturing was followed by RNA extraction, rRNA depletion, subsequent library preparation, and sequencing. Analysis was split into two parts; one to determine the enterococcal response and a separate one to determine the host response.

RNA sequencing (Fig. 2). Sequencing resulted in 5.4–29.1 million reads (10th–90th percentile) per sample. For the co-culture samples and colonic epithelium samples, 0.9–13.2 million reads (10th–90th percentile) mapped to genes from the human genome indicating large variation in read counts between the six replicates, and more importantly, that in three of the six replicates the recommended minimum of 10 million reads aligning with the eukaryotic part of the database was not reached (Fig. S3) (Westermann et al. 2017). Principal component analysis (PCA) also indicated large variation between batches and to a lesser extent variation based on culture condition (Figs S4b and S5b). Therefore, we decided to not continue with the analysis of the host response and only focus on the bacterial response during colonic epithelium colonization.

Co-culture of *E. faecium* E8202 with colonic epithelium results in altered patterns of *E. faecium* gene expression

Sequencing resulted in 5.4–29.1 million reads (10th–90th percentile) per sample. For the co-culture samples and *E. faecium* samples, 3.1–31.2 million reads (10th–90th percentile) mapped to *E. faecium* specific genes (Fig. S3). This is in accordance with the coverage used in previous studies that applied dual RNA sequencing to measure genome-wide transcriptional changes of both bacteria and host cells on bacteria (Westermann et al. 2017). The high read count numbers for housekeeping genes *gdh* (5300 normalized reads) and *gyrA* (14 800 normalized reads) additionally indicate sufficient gene coverage (Fig. S4a). The *hprt1* housekeeping gene, appeared to be transcribed in lower amounts, but was still detected in all replicates. PCA revealed that culture condition (i.e. either *E. faecium* monoculture or co-culture with human colonic epithelium) was the main driver of the observed variance in gene expression between the samples in *E. faecium* E8202 (Fig. S5a).

Compared to the control condition (here *E. faecium* grown in transwells in only cell culture differentiation medium in the same conditions as the co-cultures), and while applying batch correction, we observed a total of 498 differentially expressed *E. faecium* genes ($p_{adj} < 0.05$, fold change > 1.5, Fig. 3) in response to exposure to the colonic epithelium. From these, 238 genes were upregulated (47.8%) and 260 genes were downregulated (52.2%) (Tables S2 and S3).

Enterococcus faecium E8202 upregulated genes

Of all 238 significantly upregulated genes (Table S2), 187 (79%) genes are chromosomally located, 49 genes on plasmid_2 (21%), and one gene on plasmid_3 and one on plasmid_6.

The top 50 significantly upregulated chromosomally located genes are part of eight locus clusters. Cluster 93 represents genes that are involved in purine metabolism (EQB38_RS06220, *xpt;* EQB38_RS06235, *purE;* EQB38_RS06240, *purK*; EQB38_RS06245, *purB*; EQB38_RS06265, *purC*; EQB38_RS06270, *purS*; EQB38_RS06275, *purQ;* EQB38_RS06280, *purl*; EQB38_RS06285, *purF*; EQB38_RS06290, *purM*; EQB38_RS06295, *purN*; EQB38_RS06300, *purH*; EQB38_RS06305, *purD* EQB38_RS06310), while cluster 94 represents genes that are involved in pyrimidine metabolism (*pyrR*, EQB38_RS07020, *pyrB*, *pyrC*, *carA*, *carB*, *pyrDII*, *pyrDB*, *pyrF*, *pyrE*). In addition, a cluster of three loci, EQB38_RS02225 (lytTR family DNA-binding domain-containing protein), EQB38_RS02230 (sensor histidine kinase), and *agrB* putatively encodes a two-component system, while loci EQB38_RS14980, EQB38_RS14985, EQB38_RS14990, EQB38_RS14995 are part of a putative operon with a yet unknown function (Fig. 4 and Table S2).

In addition, the top 50 significantly upregulated genes also included chromosomal genes that are not predicted to be part of a gene operon or gene cluster representing nine loci with the following putative functions: bifunctional acetaldehyde-CoA/alcohol dehydrogenase (EQB38_RS01120), NCS2 family permease (EQB38_RS05170), amino acid permease (EQB38_RS10240), class II bacteriocin (EQB38_RS10540). Finally, EQB38_RS17170 (*sspP*), putatively encoding a C47 peptidase is localized on the 5.778 bp large plasmid_6.

E8202 plasmid_2 upregulated genes

In addition to the chromosomal located genes, 49 genes (out of 238 genes, 21%) that were upregulated are located on a 188 833 bp large plasmid, named plasmid_2 (GenBank: LR135345.1). In fact, 49/179 (27%) of plasmid_2 protein coding genes were significantly upregulated, indicating that this 188 833 bp plasmid seems to be highly responsive to the experimental conditions.

Of the 49 significantly upregulated genes, 36 genes (73%) grouped in eight gene clusters (Table S4, Fig. 4, Fig. S6a). Six genes of cluster 52 (loci EQB38_RS15745, EQB38_RS15750,

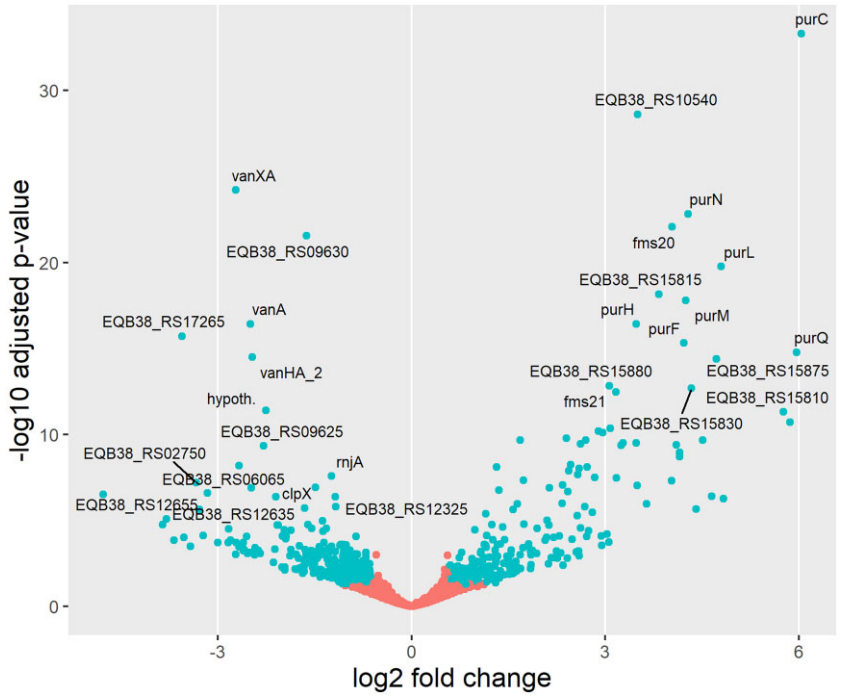

Figure 3. Volcano plot representing the significant upregulated and downregulated genes in *E. faecium* during colonization of colonic epithelium. Genes with gene ID description represent the most significant gene response in terms of fold change (*x*-axis) and consistent response between batches (*P*-value .05).

EQB38_RS15755, EQB38_RS15760, EQB38_RS15770, EQB38_RS15775) are annotated as genes belonging to the putative *pilA* (fms21) gene cluster, encoding PilA/Fms21 pili from pilin gene clusters [PGCs-1 (Hendrickx et al. 2008)]. The 16 upregulated genes (EQB38_RS15785, EQB38_RS15790, EQB38_RS15795, EQB38_RS15800, EQB38_RS15805, EQB38_RS15810, EQB38_RS15815, EQB38_RS15820, EQB38_RS15825, EQB38_RS15830, EQB38_RS15835, EQB38_RS15840, EQB38_RS15845, EQB38_RS15850, EQB38_RS15855, EQB38_RS15860) located adjacent to the *pilA* (fms21) gene cluster are predicted to be part of a conjugative type IV secretion system (Goessweiner-Mohr et al. 2013). Five upregulated genes (EQB38_RS15870, EQB38_RS15875, EQB38_RS15880, EQB38_RS15885, EQB38_RS15890) were predicted to be implicated in plasmid range, replication, and maintenance, while loci EQB38_RS16235 and EQB38_RS16240, putatively encode an ABC transporter system. A final cluster of seven upregulated genes (EQB38_RS16630, EQB38_RS16695, EQB38_RS16700, EQB38_RS16705, EQB38_RS16710, EQB38_RS16715, EQB38_RS16720) were predicted to encode a PTS system and regulatory genes).

In addition, 13 genes, not contained in larger gene clusters, were significantly upregulated (Table S4, Fig. S6a). Of these seven are encoding a putative hypothetical protein (EQB38_RS15920, EQB38_RS15950, EQB38_RS15955, EQB38_RS16050, EQB38_RS17365, EQB38_RS16450, EQB38_RS17370). The *traE* gene (EQB38_RS15705) encoding a putative ATPase is located upstream of the *pilA* (fms21) gene cluster. Furthermore, two genes (EQB38_RS16055 and EQB38_RS16485) putatively encode a DNA cytosine methyltransferase and a PBECR4 domain-containing protein, with predicted roles in plasmid maintenance. EQB38_RS16140 putatively encodes a response regulator transcription factor, while EQB38_RS16300 is predicted to encode the TnpB DNA endonuclease. Finally, EQB38_RS16335 is predicted to encode a Toll/interleukin-1 receptor (TIR)-domain-containing protein.

E8202 downregulated genes

Of all 260 significantly downregulated genes (Table S3), 251 (97%) genes are chromosomally located, while only nine genes were localized on plasmids (plasmid_2, 1 gene; plasmid_3, 4 genes; plasmid_4, 3 genes; and plasmid_7, 1 gene). This indicates that the downregulated genes were much more dominated by chromosomally located genes instead of plasmid genes than this was the case for the upregulated genes (Table S4). The four downregulated genes located on plasmid_3, *vanS*, *vanH*, *vanA*, and *vanX* are part of the *vanA* vancomycin resistance operon. Plasmid_3 is a 40,152 bp large plasmid (Genbank number NZ_LR135346.1), which has a full length rep2 replicase belonging to the Inc18 family similar to the replicase of pRE25.

In addition to the *vanA* operon, two large chromosomally encoded clusters comprising of 18 genes encompassing loci EQB38_RS12610–EQB38_RS12710 (cluster 64) and 14 genes encompassing loci (EQB38_RS12745–EQB38_RS12835) (clusters 33 and 65) both encoding phage proteins were significantly downregulated (Table S3, Fig. 4). Loci EQB38_RS02360–EQB38_RS02365 putatively encode enzymes implicated in aspartate reduction, while loci EQB38_RS09805–EQB38_RS09830 encode proteins that are part of a putative PTS. Furthermore, other genes belonging to the top 50 downregulated genes putatively encoding various cellular functions are displayed in Fig. 4 and further described in Table S3.

KEGG pathway analysis

To further understand the physiological processes encoded by differentially expresses the statistical enrichment ($p_{adj} < 0.1$, fold change > 1.5) of these *E. faecium* E8202 genes in KEGG pathways was determined. In addition of finding similarities in function based on genomic clustering, KEGG analysis also allows a genome-wide identification of genes encoding shared functions. From the resulting 498 differentially expressed genes, 335

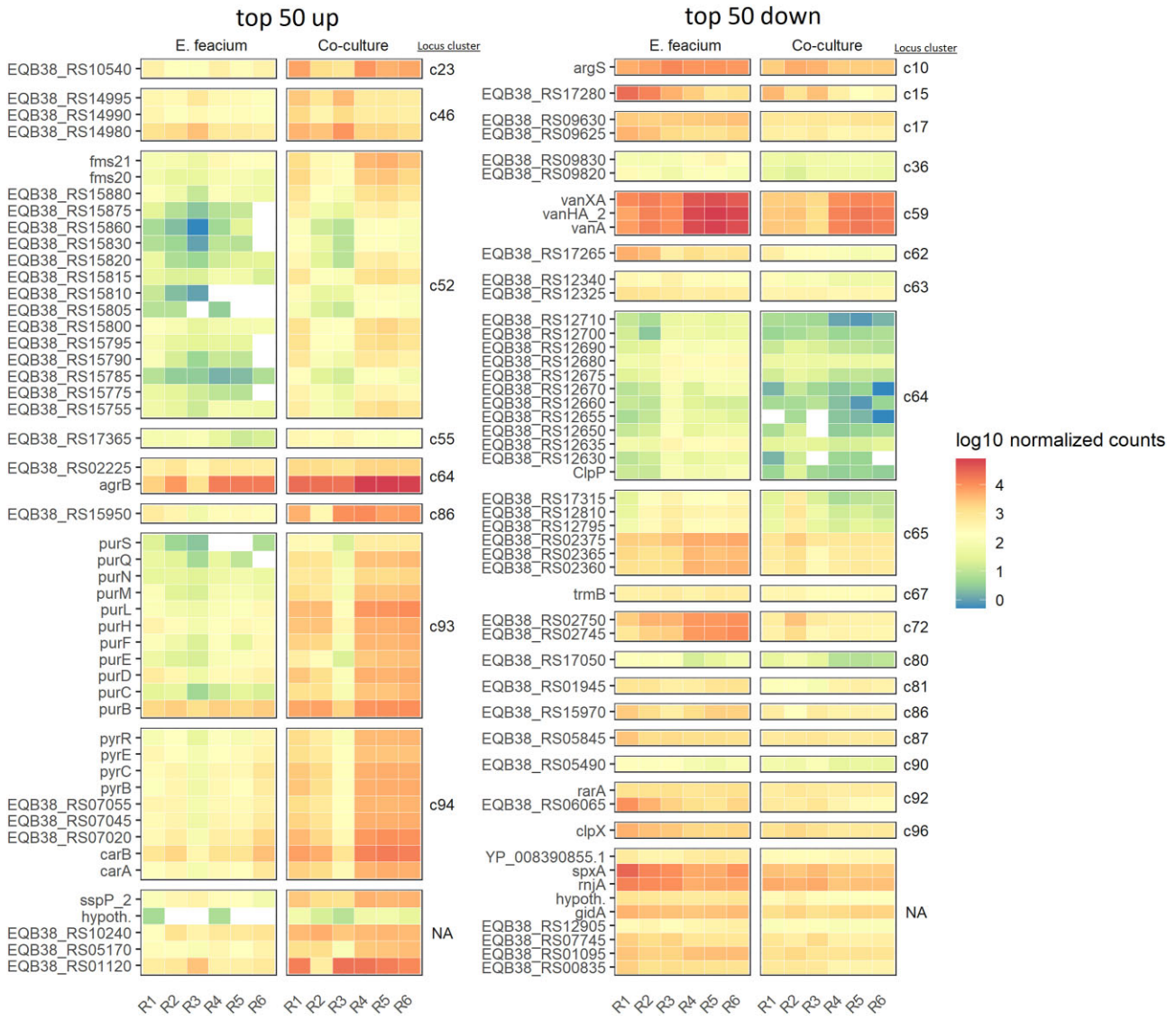

Figure 4. Differentially transcribed genes in *E. faecium* E8202 upon co-culturing with human colonic epithelium. Top 50 significant differentially expressed, upregulated, and downregulated genes, comparing control condition with co-culturing with colonic epithelium. More genes can be part of the gene clusters described on the figure, but not shown if they are in the top 50 upregulated or downregulated genes. Read counts are normalized per sample using DESeq2's size factor method. Replicates are indicated by columns, while genes are grouped per gene operon.

could be annotated with a KEGG function (Table S5). Pathway analysis revealed that these genes belong to different pathways, as shown in Fig. 5 and Table S5, such as (1) alanine, aspartate and glutamate metabolism, converting aspartate into fumarate and n-carbamoyl-l-aspartate and, additionally converting glutamine into 5-phosphoribosylamine, or alternatively into carbamoyl phosphate (*carA*, *carB*, *purA*, *purB*, *purF*, *purQ*, *pyrB*); (2) arginine biosynthesis, which applies glutamine for conversion into ammonia, followed by carbamoyl phosphate, citrulline and lastly into arginine (*arcA*, *arcB*, *arcC*); (3) purine metabolism, also converting glutamine, 5-phosphoribosylamine and possibly 5-phosphoribosyl diphosphate (PRPP) for the putative synthesis of inosinic acid (IMP) and consequently adenylic acid (AMP) (*arcC*, *purA*, *purB*, *purC*, *purD*, *purE*, *purF*, *purH*, *purL*, *purM*, *purN*, *purQ*, *purS*); (4) pyrimidine metabolism, utilizing glutamine, carbamoyl phosphate and n-carbamoyl-l-aspartate for the generation of PRPP and uridylic acid (UMP) (*carA*, *carB*, *pyrF*, *pyrDII*, *pyrB*, *pyrC*, *pyrDB*, *pyrE*, *pyrR*), and (5) fructose and mannose metabolism, including the conversion of sorbitol to fructose-6P, and conversion of mannose to mannose-6P and fructose-1P to fructose-1,6P_2 (EQB38_RS07795–EQB38_RS07920, *EQB38_RS08575*, *EQB38_RS07935*). Expression of the genes belonging to these pathways was significantly upregulated when *E. faecium* was co-cultured with colonic epithelium compared to the control condition. Lastly, we found that expression of genes involved in biosynthesis of cofactors to be upregulated, converting 2-dehydropantoate into pantoate (EQB38_RS01355), menaquinone (vitamin k1) into menaquinol, and phylloquinone (vitamin k2) into phylloquinol (EQB38_RS14695).

In contrast, KEGG based pathway analysis indicated downregulated expression of genes to be involved in (1) biosynthesis of amino acids, particularly the conversion of homocysteine into methionine, ornithine into proline, and aspartate into lysine (*lysC*, *asd*, *dapA*, *dapB*, *dapH*, *patA*, *dapF*); (2) starch and sucrose metabolism, mainly the conversion of sucrose to glucose and fructose (*crr*, *sacA*, *celB*, *sacP*, *celC*, *scrK*); (3) galactose metabolism, the

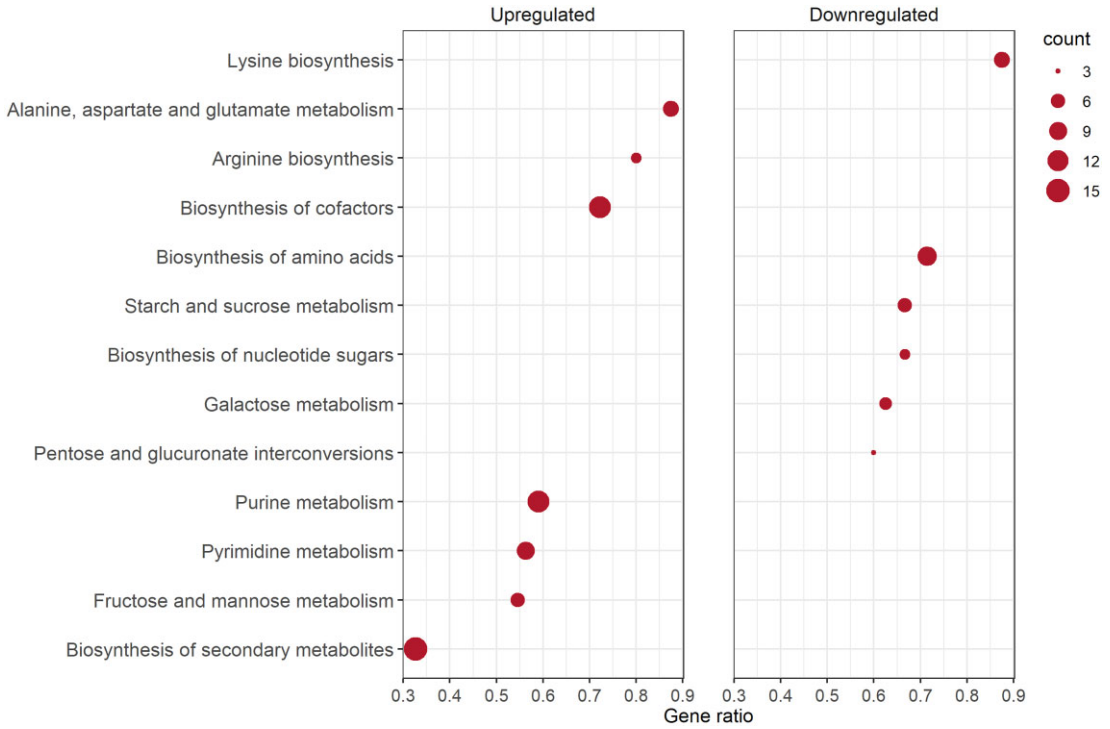

Figure 5. Gene pathway annotation of *E. faecium* genes that are differentially expressed upon co-culturing with colonic epithelium. Genes that are significantly upregulated or downregulated clustered based on KEGG gene pathways analysis using ClusterProfiler version 4.0 within R. Counts, displayed as circles, represent the number of differentially expressed genes that belong to a given pathway. Circle size is proportionate to counts. The x-axis represents the gene ratio; the proportion of differentially expressed genes to all the genes that are annotated in a specific pathway.

conversion of galactose, raffinose and stachyose (*galM*, *galK*, *galT*, *galE*, *sacA*); (4) biosynthesis of nucleotide sugars, which is a large pathway that includes galactose metabolism and also the galactose genes (*galE*, *galT*, *galK*) in addition to fructose and mannose metabolism (*scrK*); and (5) pentose and glucuronate interconversions, the conversion of altronate and galacturonate (*uxaA*, *uxaB*, *uxaC*).

E8202 plasmids_2 and 3 comparative analysis

As noted above, a sizeable fraction of the genes on plasmid_2 were differentially expressed upon interaction with human colonic epithelium relative to the control condition. To assess whether plasmids similar to E8202 plasmid_2 similar were present in the NCBI nonredundant nucleotide database a blastn search was performed with accession NZ_LR135345.1 (*E. faecium* isolate E8202 plasmid_2) as query. This resulted in 14 plasmid hits with >85% coverage and >95% identity (search date 27 April 2023) (Table 1, Fig. S6a). All 14 plasmid hits represented large repUS15 plasmids with sizes ranging between 184 907 and 239 811 bp that were contained in *E. faecium*. Twelve of the 14 strains carrying the E8202 plasmid_2 similar plasmids were of ST117, just like E8202, thus belonging to the clade A1 subpopulation of hospital adapted *E. faecium*. One strain (E6055) is ST18, also clade A1, and one strain BMT-3-2-1 is ST889, a single locus variant of ST117 and expected to cluster in *E. faecium* cladeA1. The fourteen *E. faecium* isolates with similar plasmids as E8202 plasmid_2 originated from seven different European countries and were recovered between 2010 and 2018 from hospitalized patients either from clinical sites or from faeces.

Alignment of these 14 plasmids with E8202 plasmid_2 revealed that of the 49 significantly upregulated genes, 40 (81%) were conserved in all the aligned plasmids. Plasmids pHJB-2-1_01 and pSS-3-8_01 lacked a part of the *pilA* (fms21) gene cluster (loci 2813 and 2814; *srtA* and *pilA*, respectively), while E6055 plasmid_2 lacked the *abiE* operon (loci 2842 and 2843) encoding bacterial abortive infection (Abi) system toxin anti-toxin genes that may play a role in plasmid stabilization (Dy et al. 2014). This plasmid also lacked two loci, 2854 and 2855, that putatively encode hypothetical proteins. Loci 2871 and 2872, tentatively encoding for a hypothetical protein and a DNA cytosine methyltransferase were absent in 10 of the 14 plasmids and only present, beside E8202 plasmid_2, in E7356 plasmid_2, WGS1811-4-7 plasmid_1, pE1_230, and E6055 plasmid_2. Finally, locus 2929, putatively encoding a hypothetical protein was lacking from plasmid pE1_230 (Fig. S6).

A BLAST search using the thresholds (coverage >75%; identity >95%) was performed to identify plasmids displaying similarity to E8202 plasmid_3. This resulted in only two similar plasmids: *E. faecium* plasmid pUK040_2 and *E. faecium* plasmid p4_03A17012. This indicates that E8202 plasmid_3 is not as conserved as E8202 plasmid_2. Reducing coverage thresholds to >60% resulted in 20 additional hits (Fig. S6b). This yielded in total 18 *E. faecium*, 3 *E. faecalis*, and 1 *E. durans* plasmids carrying the *vanA* operon that displayed similarity with E8202 plasmid_3 (Table 2). Alignment of these plasmids reveals that these plasmids are highly diverse with respect to size (ranging between 17 934 and 88 799), rep genes and rep families, often carrying multiple rep genes belonging to different rep families, and that particular fragments or modules were conserved with E8202 plasmid_3 (Table 2 and Fig. S6b). The highly mosaic structure of plasmid_3 might be explained by the high number of predicted IS elements (IS*1216*; ($n = 4$), IS30 and IS*6770*) and genes encoding recombinase family proteins ($n = 5$). Despite the mosaic structure, the downregulated *vanA* operon genes, *vanH*, *vanA*, *vanX*, and the upstream located regulatory genes *vanR* and *vanS* were conserved in all identified E8202 plasmid_3 similar plas-

mids. The *vanY* and *vanZ* genes, in the *vanA* transposon Tn*1546* [GenBank: M97297.1 (Arthur et al. 1993)] contained in plasmid pIP816 and located downstream of *vanX*, are missing possibly because of recombination event facilitated by the insertion of IS*1216* and IS30-type of insertion sequences downstream of *vanX*. In fact, one of the plasmids similar to E8202 plasmid_3 is pIP816 extracted from one of the first glycopeptide-resistant *E. faecium* reported (strain BM4147) and was sampled from a patient with leukaemia in France in 1986 (Leclercq et al. 1988).

Enterococcal strains carrying plasmids displaying a level of similarity with E8202 plasmid 3 represented multiple species (*E. faecium*, *E. faecalis*, and *E. durans*) and were isolated from multiple sources (humans and chicken), although most isolates were *E. faecium* (19/23) recovered from hospitalized patients of which 18 were of sequence types belonging to the hospital associated clade A1.

Discussion

Colonization and subsequent overgrowth of vancomycin resistant *E. faecium* is an important cause for subsequent infection and dissemination within and between hospitalized patients. The impact of this intestinal overgrowth on host–enterococcal interactions is not well studied. In this study, we applied an RNA sequencing approach with the aim unravel the transcriptional dynamics of both *E. faecium* and human derived colonic epithelium upon co-culturing. In our studies, we used the hospital-associated vancomycin (vanA-type) resistant *E. faecium* strain E8202, which was previously isolated from a patient during a Dutch hospital outbreak (Top et al. 2020). Our results reveal that the main transcriptional response of *E. faecium* strain E8202 to colonic epithelium involves upregulation of genes involved in pilus biogenesis, plasmid conjugation machinery, and maintenance systems located on plasmid_2 and downregulation of vancomycin resistance genes located on plasmid_3. In addition, we observed transcriptional rewiring of *E. faecium* by redirecting its metabolism towards amino acid scavenging and reduction. Unfortunately, we were not able to perform a detailed analysis of the host response, which was due to the fact that the sequence depth of replicate 4–6 was below the recommended minimum of 10 million reads, resulting in substantial sequencing batch variation (Westermann et al. 2017). This has refrained us from evaluating the response of host colonic cells upon exposure to *E. faecium*.

Co-culturing of *E. faecium* E8202 with colonic epithelium for 24 h resulted in the differentially expression of a broad array of genes. Of the upregulated genes, a substantial number were located on *E. faecium* E8202 plasmid_2. Of these genes, 22, contained in two clusters, encoded the *pilA*(*fms21*) gene cluster gene cluster and a conjugative type IV secretion system. The *pilA*(*fms21*) gene cluster encodes the genes necessary for the biosynthesis of *E. faecium* PilA (Fms21) pili (Hendrickx et al. 2008, Sillanpää et al. 2008, Kim et al. 2010). This gene cluster has previously been linked to large conjugative plasmids (Kim et al. 2010). PilA (Fms21) pili are putative adhesins that were associated with gut colonization, biofilm formation, and virulence (Kim et al. 2010, Şchiopu et al. 2023). The *pilA*(*fms21*) gene cluster is located in between genes, that are predicted to be part of a putative conjugative type IV secretion system, and that are also upregulated. This may suggest that the *pilA*(*fms21*) cluster could be part of this type IV conjugation apparatus. Although it has been thought that conjugation machines in Gram-positive species seem to differ from their Gram-negative species counterparts by lacking conjugative pili (Grohmann et al. 2018), it has also been shown that Ebp pili are implicated in interaction with neighboring cells to facilitate lateral gene transfer by conjugation (La Rosa et al. 2016). Whether the *pilA*(*fms21*) is indeed part of a conjugation apparatus in *E. faecium* remains to be investigated.

Expression of surface adhesins in Gram-positive bacteria is tightly controlled (Kreikemeyer et al. 2011). It has been shown before that PilA (Fms21) pili were expressed only when cells were grown on solid media suggesting contact-dependent pilus formation (Hendrickx et al. 2008). Also, for other Gram-positive bacteria growth condition and growth phase-dependent expression of pili has been reported (Kreikemeyer et al. 2011). In *E. faecalis*, expression of the Ebp pilus encoding locus is enhanced by the presence of bicarbonate, which might be especially relevant for the experimental setup detailed in our study as in the distal colon there is a net secretion of bicarbonate implicated in mucin expulsion from the crypt into the colonic lumen (Bourgogne et al. 2010, Birchenough et al. 2015). Still, detailed knowledge about environmental signals triggering *E. faecium* pilus expression is incomplete. Like pili expression, also the expression of conjugative type IV secretion systems in Gram-positive bacteria is tightly controlled. In general, the conjugation apparatus is not expressed until the system is induced by signaling molecules from the environment (Kohler et al. 2019). These signal molecules include small peptides that signal as a function of cell density, a process called quorum sensing. Sex pheromone-responsive plasmids, which are found in both *E. faecalis* and *E. faecium* strains and are amongst the best-studied conjugative plasmids regulated by quorum sensing (Magi et al. 2003, Goessweiner-Mohr et al. 2013, Kohler et al. 2019, Pena et al. 2019). Accumulation of *E. faecium* at the surface of colonic epithelium may have triggered the expression of both pili and the conjugation apparatus. If so, this would imply that conjugational gene exchange is enhanced at the surface of the intestinal epithelial cell lining in the gut, similarly as the finding of increased conjugative transfer in biofilms (Kelly et al. 2009).

Another set of genes located on plasmid_2 and upregulated in the presence of colon organoids encode a phosphoenolpyruvate: carbohydrate PTS sugar transport system. Bacterial PTS catalyzes the uptake and concomitant phosphorylation of various carbohydrates (Saier 2015). Expression of PTS systems is tightly controlled so that genes encoding enzymes required for uptake and metabolism of the substrate are only expressed, in fact, derepressed, when the substrate is available (Deutscher et al. 2006). The observation that expression of this PTS system is upregulated (derepressed) suggests that under these conditions the substrate for the PTS is available, likely provided by the cultured organoids, whereas this was not the case in the control condition. Recently, Huang et al. showed also upregulated PTS related genes when endogenous infected *E. faecium* isolates were grown in the presence of urine (Huang et al. 2023). Genes encoding putative regulators of the PTS located on plasmid_2 are the adjacent loci 2975 (EQB38_RS16700), encoding a putative SIS (Sugar Isomerase) domain-containing proteins and 2974 (EQB38_RS16695), tentatively encoding a sigma 54-interacting transcriptional regulator and possibly locus 2964 (EQB38_RS16630) encoding a putative GntR family transcriptional regulator (Yamamoto et al. 2001, Deutscher et al. 2006). KEGG pathways analysis also revealed changes in expression of several *E. faecium* genes implicated in starch and sugar metabolism. Specifically, genes implicated in the reduction of galactose, raffinose, and stachyose were downregulated. In contrast, genes implicated in mannose and fructose metabolism pathways were upregulated, increasing the conversions of sorbitol to fructose-6P, and conversion of mannose into mannose-6P and fructose-1P into fructose-1,6P2. The uptake and utilization of fructose, mannose, and amino sugars have been re-

ported to be linked to *E. faecium* isolates belonging to the hospital clade (clade A1) and were shown to play an important role in colonization of the intestinal tract of mice, following antibiotic treatment (Lebreton et al. 2013, Zhang et al. 2013). The increased utilization of sorbitol and glycogen suggests sources of these compounds in our model. The main known source of glycogen in our model comes from mucus secretion, mainly MUC2, though *E. faecium* is not known as a mucus degrader (Bansil and Turner 2018). Maltose and sorbitol are furthermore examples of nutrients that are utilized by specialist bacteria in the colon (Deibel et al. 1963, Le Breton et al. 2005, Sarmiento-Rubiano et al. 2007). Together, these metabolic changes suggest that they represent important functions during intestinal colonization.

In addition, plasmid_2 genes encoding an ABC transporter implicated in the uptake of ions, sugars, amino acids, and other substrates were upregulated. Genes encoding an ABC transporter involved in maltodextrin metabolism were reported to be strongly expressed during mouse intraperitoneal infection with *E. faecalis*, suggesting that this ABC transporter might be important for *E. faecalis* virulence (Muller et al. 2015). This is corroborated by the observation that inactivation of this ABC transporter in *E. faecalis* reduced enterococcal colonization (Sauvageot et al. 2017). Alternatively, ABC exporters mediate efflux toxins and antimicrobial agents, thus may contribute to antibiotic resistance (Davidson and Chen 2004).

Finally, a putative TIR domain-containing protein was upregulated. Bacterial TIR-domain-containing proteins structurally mimic host domains, which are crucial for protein–protein interaction in the TLR signaling cascade (Newman et al. 2006, Chan et al. 2009). Therefore, TIR proteins have been implicated in immune evasion. In *E. faecalis*, the TIR-domain-containing protein TcpF attenuates MyD88-mediated signaling and promotes bacterial survival within macrophages (Kraemer et al. 2014). In *E. faecium*, it has been reported that TIR-domain-containing proteins promote bacterial proliferation in human blood, indicating that TirE may contribute to *E. faecium* pathogenesis (Wagner et al. 2018). Why this locus is upregulated in this experimental setup is yet unknown and remains to be investigated.

In addition to the changes in the expression on genes present in plasmid_2, we also observed changes in gene expression of possible other virulence factors, such as proteases. Specifically, we observed upregulation of *sspP*, a putative staphopain peptidases C47, encoded on E8202 plasmid_6. Studied peptidases from the C47 family include staphopain A in staphylococci. In *Staphylococcus aureus* Staphopain A is a key mediator of *S. aureus* virulence and plays a putative role in the destruction of connective tissue, the inhibition of host immune response, and the modulation of biofilm integrity (Laarman et al. 2012, Kolar et al. 2013). It is currently unknown the role of *sspP* in enterococci. In contrast, expression of *clpP* and *clpX*, both ATP-dependent proteases, was downregulated (Roy et al. 2019). *clpP* and *clpX* are important in bacterial growth and are part of the cellular protein quality control systems by refolding or degrading damaged proteins (Moreno-Cinos et al. 2019). Upregulation of *clpP* was observed in *E. faecalis* as a result of cell stress and resulted in the downregulation of pyrimidine metabolism genes *pyrE*, *pyrC*, and *pyrF* (Zheng et al. 2020). In concordance with this finding, downregulation of *clpP* in *E. faecium* E8202 co-occurred with upregulation of genes implicated in pyrimidine metabolism upon co-culturing with colonic epithelium, including pyrimidine metabolism genes *pyrE* and *pyrC*. In addition, genes *pyrB* and *pyrR* were upregulated in our study, as well as purine metabolism genes *purC*, *purD*, *purF*, *purH*, *purL*, *purM*, *purN*, *purQ*, and *purS*. Lim et al. compared gene expression during biofilm-formation with gene expression of cells in the planktonic phase using a vanA-type *E. faecium* strain (Lim et al. 2017). Although they observed a downregulation of *clp* protease in biofilm cells relative to planktonic cells, they did not report changes in the expression of pyrimidine metabolism genes. In *S. aureus*, the purine biosynthesis gene *purF* has been shown to regulate cell growth, biofilm formation and to play a key role in persistent methicillin-resistant *S. aureus* bacteraemia (Li et al. 2018, 2021). It remains to be investigated if *purF* could play a role in biofilm formation in enterococci as well and if this gene is also implicated in regulation of expression of pilli genes. It is intriguing that some similarities seem to exist in the transcriptional profile observed in *E. faecium* when co-cultured with human colonic epithelium and when grown in biofilms.

KEGG pathway analysis revealed a major shift in gene expression leading to a reconfiguration in metabolic pathways for energy supply. Since most of the easily accessible nutrients and carbon sources are absorbed in the small intestines, the microbiota of the colon is commonly composed of bacteria designed to salvage energy and nutrients from alternative sources. Some of these have evolved to salvage amino acids, purines, and pyrimidines as primary sources of carbon, nitrogen, and energy, similar to the response of *E. faecium* in our study (Srivastava et al. 2011, Hartwich et al. 2012, Dai et al. 2015, Wang et al. 2020). Colonocytes are able to metabolize glutamine into glutamate, aspartate, alanine, and lactate, potentially explaining why these amino acids are available for *E. faecium* (Darcy-Vrillon et al. 1993, Blachier et al. 2009). It is unclear if *E. faecium* competes for amino acids with the colonocytes in our model, or if *E. faecium* contributes to conversion pathways, for instance, by the generation of arginine. Lim et al. observed a downregulation of the arginine deiminase system (*arcA*, *arcB*, *rc*) in biofilm forming vanA-type vancomycin resistant *E. faecium* when compared to *E. faecium* grown in the planktonic phase (Lim et al. 2017). This is in contrast with our findings and also with their own expectations. They describe that an increase in arginine expression is expected during biofilm development, since it is an alternative energy source when sugars are depleted. While salvage pathways like those of amino acids can generally result in the production of beneficial short chain fatty acids, they are also known to create by-products that act as toxins to host cells, like indoles, phenols, and amines (Potrykus et al. 2008). The increased reduction of glutamine by *E. faecium* may result in the production toxic ammonia. Accumulation of ammonia is known to disrupt tight junctions of host cells and seems a possible way for pathogens to disrupt the barrier function of the intestines (Yokoo et al. 2021). Disruption of tight junctions in the presence of *E. faecium* was also previous observed by Hendrickx et al. in the mouse gut colonization *in vivo* model (Hendrickx et al. 2015). However, in our study, we also observed that during *E. faecium* and colonic epithelium co-culturing the arginine synthesis pathway of *E. faecium* is upregulated, which, through the activation of the urea cycle, would result in the reduction of ammonia. Whether or not ammonia is accumulated during *E. faecium* and colonic epithelium co-culturing is unknown and remains to be investigated.

Finally, we observed a downregulation of vancomycin resistance genes encoded by E8202 plasmid_3 (*vanH*, *vanA*, *vanX*) and in lesser degree of *vanS*, upon co-culture with colonic epithelium. The *vanS* gene is a sensor histidine kinase that can detect vancomycin and forms a two-component system together with *vanR*. The *vanR* gene encodes the response regulator that regulates the expression of the *vanH*, *vanA*, and *vanX* vancomycin resistance genes (Arthur et al. 1997). The exact mechanism by which *vanS* detects vancomycin is still unknown. It is speculated that van-

comycin is detected directly or that downstream effect of vancomycin activity, such as the accumulation of lipid II, is being sensed (Guffey and Loll 2021). In our experiments, culture media was not supplemented with vancomycin, and vancomycin can therefore not be responsible for changes in the expression of vancomycin resistance genes. One possibility is that membrane stress is responsible for the observed changes in expression. If this were the case, this would mean that *E. faecium* grown in the control condition should endure more membrane stress than the condition with colonic epithelium, resulting in the observed downregulation of vancomycin resistance genes during co-culturing. Although the exact signals that control the expression of the *vanA* operon in this study are not known, this is, to our knowledge, the first time that it is shown that upon interaction with human host cells representative of the human gut epithelium expression of vancomycin resistance genes is not induced in *E. faecium*. It is yet unknown if non-induction or downregulation of vancomycin resistance genes functions as a way to preserve energy or if it has additional functions. Moreover, non-induction or downregulation of the *vanA* operon could be part of larger structural changes in the cell wall, which potentially affects host–pathogen interaction (Chang et al. 2018). Together, these results suggest that the vanA-type vancomycin resistant *E. faecium* strain E8202 used in this study, remains susceptible to vancomycin upon colonization on colonic epithelium. Future studies in which media are supplemented with vancomycin, might reveal *vanA* gene operon driven changes in host–pathogen interaction.

The 188 833 bp large conjugative E8202 plasmid 2 that encoded over a quarter of the genes that were upregulated when *E. faecium* E8202 was co-cultured with human colonic epithelial cells was highly conserved among *E. faecium*. Over 80% of these upregulated genes were found to be contained on 14 similar large conjugative *E. faecium* plasmids and these plasmids were also contained in *E. faecium* strains belonging to the hospital subpopulation clade A1. This suggests that these types of large conjugative plasmids may contribute to gut colonization and proliferation of *E. faecium* in hospitalized patients, thus to the ecological success of this subpopulation in the hospital environment. This is in line with the previous observation that particularly plasmid sequences (the plasmidome) contribute to niche adaptation, including hospitals (Arredondo-Alonso et al. 2020). In contrast, E8202 plasmid_3 on which the downregulated *vanA* operon is located is less conserved among *E. faecium* or other *Enterococcus* species, indicating that this plasmid seems to be more modular. The observation that the *vanA* operon on E8202 plasmid_3 was surrounded by insertion sequences and recombinase encoding genes (Fig. S6b) suggests that this operon can frequently be transferred between plasmids. Linkage of the *vanA* operon to a diverse range of plasmids with a high degree of mosaicism has also been reported before, and proposed to importantly contribute local adaptation of *E. faecium* clones (Rosvoll et al. 2010, Wardal et al. 2017).

To conclude, RNA sequencing of a confluent monolayer of human colonic epithelium co-cultured with vancomycin resistant *E. faecium* revealed an elaborate and diverse bacterial response. When exposed to the colonic epithelium, colonization of *E. faecium* seems to be facilitated by pili expression and downregulation of vancomycin resistance operon, while metabolism switched to amino acid scavenging and reduction. In addition, upregulation of conjugative type IV secretion system and various plasmid host range, maintenance, and replication systems suggest increased plasmid dissemination in *E. faecium* upon interaction with human colonic epithelium, which can contribute to the increased relative abundance and intestinal outgrowth of clade A1 *E. faecium* in hospitalized patients. Future studies involving additional *E. faecium* strains and isogenic mutants are required to confirm the results obtained here and to mechanistically study the role of the identified cell responses in host–pathogen interaction. Increasing the knowledge on the mechanisms implicated in *E. faecium*–host interaction may help to design novel anti-infectivity strategies.

Supplementary data

Supplementary data is available at *FEMSMC Journal* online.

Conflict of interest: None declared.

Funding

This work was supported by the Netherlands Centre of One Health (NCOH metagenome call).

Data availability

The 18 RNA sequencing files have been deposited in the European Nucleotide Archive repository under the study accession PRJEB74040. R scripts to reproduce the analysis reported in this study can be found at https://gitlab.com/PB_Stege/efm_rna_seq_analysis.

References

Arredondo-Alonso S, Top J, McNally A *et al.* Plasmids shaped the recent emergence of the major nosocomial pathogen *Enterococcus faecium*. *mBio* 2020;**11**:e03284–19.

Arthur M, Depardieu F, Gerbaud G *et al.* The VanS sensor negatively controls VanR-mediated transcriptional activation of glycopeptide resistance genes of Tn*1546* and related elements in the absence of induction. *J Bacteriol* 1997;**179**:97–106.

Arthur M, Molinas C, Depardieu F *et al.* Characterization of Tn*1546*, a Tn3-related transposon conferring glycopeptide resistance by synthesis of depsipeptide peptidoglycan precursors in *Enterococcus faecium* BM4147. *J Bacteriol* 1993;**175**:117–27.

Bansil R, Turner BS. The biology of mucus: composition, synthesis and organization. *Adv Drug Deliv Rev* 2018;**124**:3–15.

Birchenough GM, Johansson ME, Gustafsson JK *et al.* New developments in goblet cell mucus secretion and function. *Mucosal Immunol* 2015;**8**:712–9.

Blachier F, Boutry C, Bos C *et al.* Metabolism and functions of L-glutamate in the epithelial cells of the small and large intestines. *Am J Clin Nutr* 2009;**90**:814s–21s.

Bourgogne A, Thomson LC, Murray BE. Bicarbonate enhances expression of the endocarditis and biofilm associated pilus locus, *ebpR-ebpABC*, in *Enterococcus faecalis*. *BMC Microbiol* 2010;**10**:17.

Carattoli A, Zankari E, García-Fernández A *et al.* In silico detection and typing of plasmids using PlasmidFinder and plasmid multilocus sequence typing. *Antimicrob Agents Chemother* 2014;**58**:3895–903.

Chan SL, Low LY, Hsu S *et al.* Molecular mimicry in innate immunity: crystal structure of a bacterial TIR domain. *J Biol Chem* 2009;**284**:21386–92.

Chang JD, Wallace AG, Foster EE *et al.* Peptidoglycan compositional analysis of *Enterococcus faecalis* biofilm by stable isotope labeling by amino acids in a bacterial culture. *Biochemistry* 2018;**57**:1274–83.

Chilambi GS, Nordstrom HR, Evans DR *et al.* Evolution of vancomycin-resistant *Enterococcus faecium* during coloniza-

tion and infection in immunocompromised pediatric patients. *Proc Natl Acad Sci USA* 2020;**117**:11703–14.

Dai Z, Wu Z, Hang S *et al.* Amino acid metabolism in intestinal bacteria and its potential implications for mammalian reproduction. *Mol Hum Reprod* 2015;**21**:389–409.

Darcy-Vrillon B, Morel MT, Cherbuy C *et al.* Metabolic characteristics of pig colonocytes after adaptation to a high fiber diet. *J Nutr* 1993;**123**:234–43.

Davidson AL, Chen J. ATP-binding cassette transporters in bacteria. *Annu Rev Biochem* 2004;**73**:241–68.

Deibel RH, Lake DE, Niven CF. Physiology of the Enterococci as related to their taxonomy. *J Bacteriol* 1963;**86**:1275–82.

de Maat V, Stege PB, Dedden M *et al.* CRISPR-Cas9-mediated genome editing in vancomycin-resistant *Enterococcus faecium*. *FEMS Microbiol Lett* 2019;**366**:fnz256.

de Regt MJ, van der Wagen LE, Top J *et al.* High acquisition and environmental contamination rates of CC17 ampicillin-resistant *Enterococcus faecium* in a Dutch hospital. *J Antimicrob Chemother* 2008;**62**:1401–6.

Deutscher J, Francke C, Postma PW. How phosphotransferase system-related protein phosphorylation regulates carbohydrate metabolism in bacteria. *Microbiol Mol Biol Rev* 2006;**70**:939–1031.

Dobin A, Davis CA, Schlesinger F *et al.* STAR: ultrafast universal RNA-seq aligner. *Bioinformatics* 2013;**29**:15–21.

Dy RL, Przybilski R, Semeijn K *et al.* A widespread bacteriophage abortive infection system functions through a Type IV toxin-antitoxin mechanism. *Nucleic Acids Res* 2014;**42**:4590–605.

Goessweiner-Mohr N, Arends K, Keller W *et al.* Conjugative type IV secretion systems in Gram-positive bacteria. *Plasmid* 2013;**70**:289–302.

Grant JR, Enns E, Marinier E *et al.* Proksee: in-depth characterization and visualization of bacterial genomes. *Nucleic Acids Res* 2023;**51**:W484–w492.

Grohmann E, Christie PJ, Waksman G *et al.* Type IV secretion in Gram-negative and Gram-positive bacteria. *Mol Microbiol* 2018;**107**:455–71.

Guffey AA, Loll PJ. Regulation of resistance in vancomycin-resistant *Enterococci*: the VanRS two-component system. *Microorganisms* 2021;**9**: 2026.

Hartwich K, Poehlein A, Daniel R. The purine-utilizing bacterium *Clostridium acidurici* 9a: a genome-guided metabolic reconsideration. *PLoS One* 2012;**7**:e51662.

Hendrickx AP, Top J, Bayjanov JR *et al.* Antibiotic-driven dysbiosis mediates intraluminal agglutination and alternative segregation of *Enterococcus faecium* from the intestinal epithelium. *mBio* 2015;**6**:e01346–15.

Hendrickx APA, Bonten MJM, van Luit-Asbroek M *et al.* Expression of two distinct types of pili by a hospital-acquired *Enterococcus faecium* isolate. *Microbiology* 2008;**154**:3212–23.

Huang G, Zhou Y, Cheng H *et al.* Genome and transcriptome analysis of *Enterococcus faecium* from intestinal colonization and *Enterococcus faecium* from urinary tract infection. *Front Microbiol* 2023;**14**:1273949.

Jiao S, Li X, Yu H *et al.* In situ enhancement of surfactin biosynthesis in *Bacillus subtilis* using novel artificial inducible promoters. *Biotechnol Bioeng* 2017;**114**:832–42.

Jung P, Sato T, Merlos-Suárez A *et al.* Isolation and in vitro expansion of human colonic stem cells. *Nat Med* 2011;**17**:1225–7.

Kelly BG, Vespermann A, Bolton DJ. The role of horizontal gene transfer in the evolution of selected foodborne bacterial pathogens. *Food Chem Toxicol* 2009;**47**:951–68.

Kim DS, Singh KV, Nallapareddy SR *et al.* The *fms21* (*pilA*)-*fms20* locus encoding one of four distinct pili of *Enterococcus faecium* is harboured on a large transferable plasmid associated with gut colonization and virulence. *J Med Microbiol* 2010;**59**:505–7.

Kohler V, Keller W, Grohmann E. Regulation of Gram-positive conjugation. *Front Microbiol* 2019;**10**:1134.

Kolar SL, Ibarra JA, Rivera FE *et al.* Extracellular proteases are key mediators of *Staphylococcus aureus* virulence via the global modulation of virulence-determinant stability. *Microbiologyopen* 2013;**2**:18–34.

Kraemer TD, Quintanar Haro OD, Domann E *et al.* The TIR domain containing locus of *Enterococcus faecalis* is predominant among urinary tract infection isolates and downregulates host inflammatory response. *Int J Microbiol* 2014;**2014**:918143.

Kreikemeyer B, Gámez G, Margarit I *et al.* Genomic organization, structure, regulation and pathogenic role of pilus constituents in major pathogenic Streptococci and Enterococci. *Int J Med Microbiol* 2011;**301**:240–51.

Laarman AJ, Mijnheer G, Mootz JM *et al.* *Staphylococcus aureus* Staphopain A inhibits CXCR2-dependent neutrophil activation and chemotaxis. *Embo J* 2012;**31**:3607–19.

La Rosa SL, Montealegre MC, Singh KV *et al.* *Enterococcus faecalis* Ebp pili are important for cell-cell aggregation and intraspecies gene transfer. *Microbiology (Reading)* 2016;**162**:798–802.

Lebreton F, van Schaik W, McGuire AM *et al.* Emergence of epidemic multidrug-resistant *Enterococcus faecium* from animal and commensal strains. *mBio* 2013;**4**:e00534–13.

Le Breton Y, Pichereau V, Sauvageot N *et al.* Maltose utilization in *Enterococcus faecalis*. *J Appl Microbiol* 2005;**98**:806–13.

Leclercq R, Derlot E, Duval J *et al.* Plasmid-mediated resistance to vancomycin and teicoplanin in *Enterococcus faecium*. *N Engl J Med* 1988;**319**:157–61.

Li L, Abdelhady W, Donegan NP *et al.* Role of purine biosynthesis in persistent methicillin-resistant *Staphylococcus aureus* infection. *J Infect Dis* 2018;**218**:1367–77.

Li L, Li Y, Zhu F *et al.* New mechanistic insights into purine biosynthesis with second messenger c-di-AMP in relation to biofilm-related persistent methicillin-resistant *Staphylococcus aureus* infections. *mBio* 2021;**12**:e0208121.

Lim SY, Teh CSJ, Thong KL. Biofilm-related diseases and Omics: global transcriptional profiling of *Enterococcus faecium* reveals different gene expression patterns in the biofilm and planktonic Cells. *OMICS* 2017;**21**:592–602.

Love MI, Huber W, Anders S. Moderated estimation of fold change and dispersion for RNA-seq data with DESeq2. *Genome Biol* 2014;**15**:550.

Magi G, Capretti R, Paoletti C *et al.* Presence of a vanA-carrying pheromone response plasmid (pBRG1) in a clinical isolate of *Enterococcus faecium*. *Antimicrob Agents Chemother* 2003;**47**:1571–6.

Magruder M, Sholi AN, Gong C *et al.* Gut uropathogen abundance is a risk factor for development of bacteriuria and urinary tract infection. *Nat Commun* 2019;**10**:5521.

McClintock SD, Attili D, Dame MK *et al.* Differentiation of human colon tissue in culture: effects of calcium on trans-epithelial electrical resistance and tissue cohesive properties. *PLoS One* 2020;**15**:e0222058.

Moreno-Cinos C, Goossens K, Salado IG *et al.* ClpP protease, a promising antimicrobial target. *Int J Mol Sci* 2019;**20**:2232.

Moriya Y, Itoh M, Okuda S *et al.* KAAS: an automatic genome annotation and pathway reconstruction server. *Nucleic Acids Res* 2007;**35**:W182–5.

Muller C, Cacaci M, Sauvageot N *et al.* The intraperitoneal transcriptome of the opportunistic pathogen *Enterococcus faecalis* in mice. *PLoS One* 2015;**10**:e0126143.

N Coleman. A new open-source superfolding green fluorescent protein: Free-Use GFP (fuGFP). 2019.

Newman RM, Salunkhe P, Godzik A *et al.* Identification and characterization of a novel bacterial virulence factor that shares homology with mammalian Toll/interleukin-1 receptor family proteins. *Infect Immun* 2006;**74**:594–601.

Pena RT, Blasco L, Ambroa A *et al.* Relationship between quorum sensing and secretion systems. *Front Microbiol* 2019;**10**:1100.

Potrykus J, White RL, Bearne SL. Proteomic investigation of amino acid catabolism in the indigenous gut anaerobe *Fusobacterium varium*. *Proteomics* 2008;**8**:2691–703.

R Core Team T. R: A Language and Environment for Statistical Computing. 2020.

Rosvoll TC, Pedersen T, Sletvold H *et al.* PCR-based plasmid typing in *Enterococcus faecium* strains reveals widely distributed pRE25-, pRUM-, pIP501- and pHTbeta-related replicons associated with glycopeptide resistance and stabilizing toxin-antitoxin systems. *FEMS Immunol Med Microbiol* 2010;**58**:254–68.

Roy S, Zhu Y, Ma J *et al.* Role of ClpX and ClpP in *Streptococcus suis* serotype 2 stress tolerance and virulence. *Microbiol Res* 2019;**223–225**:99–109.

Ruiz-Garbajosa P, de Regt M, Bonten M *et al.* High-density fecal *Enterococcus faecium* colonization in hospitalized patients is associated with the presence of the polyclonal subcluster CC17. *Eur J Clin Microbiol Infect Dis* 2012;**31**:519–22.

Saier MH. The bacterial phosphotransferase system: new frontiers 50 years after Its discovery. *J Mol Microbiol Biotechnol* 2015;**25**:73–8.

Sarmiento-Rubiano LA, Zúñiga M, Pérez-Martínez G *et al.* Dietary supplementation with sorbitol results in selective enrichment of lactobacilli in rat intestine. *Res Microbiol* 2007;**158**:694–701.

Sauvageot N, Mokhtari A, Joyet P *et al. Enterococcus faecalis* uses a phosphotransferase system permease and a host colonization-related ABC transporter for maltodextrin uptake. *J Bacteriol* 2017;**199**:e00878–16.

Şchiopu P, Toc DA, Colosi IA *et al.* An overview of the factors involved in biofilm production by the *Enterococcus* Genus. *Int J Mol Sci* 2023;**24**:11577.

Seemann T. Prokka: rapid prokaryotic genome annotation. *Bioinformatics* 2014;**30**:2068–9.

Sillanpää J, Nallapareddy SR, Prakash VP *et al.* Identification and phenotypic characterization of a second collagen adhesin, Scm, and genome-based identification and analysis of 13 other predicted MSCRAMMs, including four distinct pilus loci, in *Enterococcus faecium*. *Microbiology* 2008;**154**:3199–211.

Srivastava M, Mallard C, Barke T *et al.* A selenium-dependent xanthine dehydrogenase triggers biofilm proliferation in *Enterococcus faecalis* through oxidant production. *J Bacteriol* 2011;**193**:1643–52.

Stein-Thoeringer CK, Nichols KB, Lazrak A *et al.* Lactose drives *Enterococcus* expansion to promote graft-versus-host disease. *Science* 2019;**366**:1143–9.

Taboada B, Estrada K, Ciria R *et al.* Operon-mapper: a web server for precise operon identification in bacterial and archaeal genomes. *Bioinformatics* 2018;**34**:4118–20.

Taur Y, Xavier JB, Lipuma L *et al.* Intestinal domination and the risk of bacteremia in patients undergoing allogeneic hematopoietic stem cell transplantation. *Clin Infect Dis* 2012;**55**:905–14.

Top J, Arredondo-Alonso S, Schürch AC *et al.* Genomic rearrangements uncovered by genome-wide co-evolution analysis of a major nosocomial pathogen, *Enterococcus faecium*. *Microb Genom* 2020;**6**:mgen000488.

Ubeda C, Taur Y, Jenq RR *et al.* Vancomycin-resistant *Enterococcus* domination of intestinal microbiota is enabled by antibiotic treatment in mice and precedes bloodstream invasion in humans. *J Clin Invest* 2010;**120**:4332–41.

Vonk AM, van Mourik P, Ramalho AS *et al.* Protocol for application, standardization and validation of the forskolin-induced swelling assay in cystic fibrosis human colon organoids. *STAR Protoc* 2020;**1**:100019.

Wagner TM, Janice J, Paganelli FL *et al. Enterococcus faecium* TIR-domain genes are part of a gene cluster which promotes bacterial survival in blood. *Int J Microbiol* 2018;**2018**:1435820.

Wang B, Grant RA, Laub MT. ppGpp coordinates nucleotide and amino-acid synthesis in *E. coli* during starvation. *Mol Cell* 2020;**80**:29–42.e10.

Wardal E, Kuch A, Gawryszewska I *et al.* Diversity of plasmids and Tn*1546*-type transposons among VanA *Enterococcus faecium* in Poland. *Eur J Clin Microbiol Infect Dis* 2017;**36**:313–28.

Westermann AJ, Barquist L, Vogel J. Resolving host-pathogen interactions by dual RNA-seq. *PLoS Pathog* 2017;**13**:e1006033.

WHO. World Health Organization (WHO) Global Priority List of Antibiotic-Resistant Bacteria to Guide Research, Discovery, and Development of New Antibiotics. 2017.

Wickham. ggplot2 Elegant Graphics for Data Analysis. 2016.

Willems RJ, Top J, van Santen M *et al.* Global spread of vancomycin-resistant *Enterococcus faecium* from distinct nosocomial genetic complex. *Emerg Infect Dis* 2005;**11**:821–8.

Yamamoto H, Serizawa M, Thompson J *et al.* Regulation of the *glv* operon in *Bacillus subtilis*: yfiA (GlvR) is a positive regulator of the operon that is repressed through CcpA and cre. *J Bacteriol* 2001;**183**:5110–21.

Yokoo K, Yamamoto Y, Suzuki T. Ammonia impairs tight junction barriers by inducing mitochondrial dysfunction in Caco-2 cells. *FASEB J* 2021;**35**:e21854.

Yu G, Wang LG, Han Y *et al.* clusterProfiler: an R package for comparing biological themes among gene clusters. *OMICS* 2012;**16**:284–7.

Zachos NC, Kovbasnjuk O, Foulke-Abel J *et al.* Human enteroids/colonoids and intestinal organoids functionally recapitulate normal intestinal physiology and pathophysiology. *J Biol Chem* 2016;**291**:3759–66.

Zhang X, de Maat V, Guzmán Prieto AM *et al.* RNA-seq and Tn-seq reveal fitness determinants of vancomycin-resistant *Enterococcus faecium* during growth in human serum. *Bmc Genomics [Electronic Resource]* 2017;**18**:893.

Zhang X, Top J, de Been M *et al.* Identification of a genetic determinant in clinical *Enterococcus faecium* strains that contributes to intestinal colonization during antibiotic treatment. *J Infect Dis* 2013;**207**:1780–6.

Zheng J, Wu Y, Lin Z *et al.* ClpP participates in stress tolerance, biofilm formation, antimicrobial tolerance, and virulence of *Enterococcus faecalis*. *BMC Microbiol* 2020;**20**:30.

Zhu A, Ibrahim JG, Love MI. Heavy-tailed prior distributions for sequence count data: removing the noise and preserving large differences. *Bioinformatics* 2019;**35**:2084–92.

Zomer-van Ommen DD, de Poel E, Kruisselbrink E *et al.* Comparison of ex vivo and in vitro intestinal cystic fibrosis models to measure CFTR-dependent ion channel activity. *J Cyst Fibros* 2018;**17**:316–24.

Received 31 January 2024; **revised** 27 March 2024; **accepted** 6 May 2024